Published in final edited form as:
Mol Genet Metab. 2010 June ; 100(2): 149–154. doi:10.1016/j.ymgme.2010.03.005.

OPA3, mutated in 3-methylglutaconic aciduria type III, encodes two transcripts targeted primarily to mitochondria

Marjan Huizing[a,*], **Heidi Dorward**[a], **Lien Ly**[a], **Enriko Klootwijk**[a,b], **Robert Kleta**[b], **Flemming Skovby**[c], **Wuhong Pei**[a], **Benjamin Feldman**[a], **William A. Gahl**[a], and **Yair Anikster**[d]

[a]Medical Genetics Branch, National Human Genome Research Institute, National Institutes of Health, Bethesda, Maryland 20892, USA

[b]Centre for Nephrology, University College London, UK

[c]Department of Clinical Genetics, Copenhagen University Hospital, Copenhagen, Denmark

[d]Metabolic Disease Unit, Safra Children's Hospital, Sheba Medical Centre, Sackler Medical School, Tel Aviv University, Tel-Hashomer, Israel

Abstract

3-Methylglutaconicaciduria type III (3-MGCA type III), caused by recessive mutations in the 2-exon gene *OPA3*, is characterized by early-onset bilateral optic atrophy, later-onset extrapyramidal dysfunction, and increased urinary excretion of 3-methylglutaconic acid and 3-methylglutaric acid. Here we report the identification of a novel third *OPA3* coding exon, the apparent product of a segmental duplication event, resulting in two gene transcripts, *OPA3A* and *OPA3B*. *OPA3A* deficiency (as in optic atrophy type 3) causes up-regulation of *OPA3B*. OPA3 protein function remains unknown, but it contains a putative mitochondrial leader sequence, mitochondrial sorting signal and a peroxisomal sorting signal. Our green fluorescent protein tagged OPA3 expression studies found its localization to be predominantly mitochondrial. These findings thus place the cellular metabolic defect of 3-MGCA type III in the mitochondrion rather than the peroxisome and implicate loss of *OPA3A* rather than gain of *OPA3B* in disease etiology.

Introduction

3-Methylglutaconicaciduria type III (3-MGCA type III; MIM 258501), also called Costeff optic atrophy syndrome, or Optic atrophy type 3 (OPA3), is an autosomal recessive neuro-ophthalmologic syndrome that consists of early-onset bilateral optic atrophy and late development of spasticity, extrapyramidal dysfunction and occasionally cognitive deficit [1-3]. Urinary excretion of the branched-chain organic acids 3-methylglutaconic acid (3-MGC) and 3-methylglutaric acid (3-MGR) are increased in 3-MGCA type III patients [4].

The occurrence of 3-MGCA type III in approximately 40 patients of Iraqi-Jewish origin [3] assisted in mapping the disease to 19q13.2-q13.3 [5]. In 2001, we identified the causative gene, *OPA3* [6]. *OPA3* consists of two exons and encodes for a 179-amino acid protein (OPA3) of unknown function, containing putative mitochondrial N-terminal and peroxisomal C-terminal

* **Corresponding author:** NHGRI/NIH 10 Center Drive, MSC 1851 Bld 10, Rm 10C103 Bethesda, MD 20892 Tel.: +1 (301) 402 2797 Fax: +1 (301) 480 7825 mhuizing@mail.nih.gov .

sorting signals [6]. All patients of Iraqi-Jewish origin are homozygous for a splice site founder mutation, c.143-1G>C (IVS1-1G>C), which abolishes mRNA expression in fibroblasts [6]. We subsequently identified another novel *OPA3* mutation, an in-frame 18-bp deletion in exon 2, c.320_337del (p.Q108_E113del), in a Kurdish-Turkish patient [7]. Recently, a third *OPA3* mutation was identified in a patient of Asian (Indian) origin; a nonsense c.415C>T (p.Q139X) mutation [8].

Two *OPA3* mutations, G93S and Q105E, result in a rare dominant disorder (ADOAC; MIM 165300) involving optic atrophy, cataracts and extrapyramidal signs [9,10]. The ADOAC phenotype may reflect a dominant negative effect, since heterozygous carriers of the Iraqi-Jewish loss of function founder mutation (c.143-1G>C) do not show a clinical phenotype. Similarly, a recently reported murine model harboring an L122P mutation in the heterozygous state appears normal [11].

The function of the OPA3 protein and how its deficiency causes the clinical symptoms and 3-methylglutaconic aciduria in 3-MGCA type III patients remain enigmatic. Here we report a comprehensive study of the *OPA3* gene and its translated protein. We identified a third exon and an alternate transcript of *OPA3* and determined its expression in various tissues and in 3-MGCA type III patients. We performed expression studies in fibroblasts with green fluorescent protein (GFP)-tagged OPA3 and explore mitochondrial and peroxisomal localization. We also imaged the localization, shape and inter-organellar interactions of mitochondria and peroxisomes in normal and 3-MGCA type III patients' cells.

Methods

Patients and cells

Patients samples were enrolled under the NIH protocol "Diagnosis and Treatment of Patients with Inborn Errors of Metabolism" (www.clinicaltrials.gov, trial NCT00369421), approved by the National Human Genome Research Institute's Institutional Review Board. Each patient gave written informed consent, in accordance with the Declaration of Helsinki. Skin fibroblasts were grown in Dulbecco's modified Eagle medium supplemented with 10% fetal bovine serum containing 100 U/ml penicillin and 0.1 mg/ml streptomycin.

OPA3 gene expression

RNA was isolated from cultured fibroblasts using the Trizol reagent (Invitrogen Life Technologies, Carlsbad, CA), and reversely transcribed into cDNA using the SuperScript™ First-Strand Synthesis System for RT-PCR (Invitrogen Life Technologies, Carlsbad, CA). Tissue-specific human cDNAs were obtained from BD-Biosciences (Bedford, MA) as a multiple tissue cDNA panel. Primers were designed to distinguish between the splice forms; a common forward primer in exon 1 (5′-GCAAGGTTGCGCGTGCCCTGTGAG-3′) was combined with a reverse primer specific for exon 2 (5′-GGCCACGTTAGGTACATAGGCCATG-3′) to amplify *OPA3A* (625-bp fragment), or with a reverse primer specific for exon 3 (5′-GTTCCACCTGCAGGAGGCGGA-3′) to amplify *OPA3B* (795-bp fragment). PCR amplifications were performed under standard conditions.

For LINE-1 transposon identification, Repeat Masker (http://repeatmasker.org/) and Tandem Repeats Finder (http://tandem.bu.edu/trf/trf.html) were used.

For real-time quantitative PCR, exon-specific primer-probe assays were designed by the ABI Assay-by-Design service (Applied Biosystems, Foster City, CA; sequences available upon request). PCR amplifications on DNA-free RNA (DNA-*free*™ DNase, Ambion, Austin, TX) from patient and control fibroblasts were carried out on an ABI PRISM 7900 HT Sequence

Detection System (Applied Biosystems, Foster City, CA). Results were analyzed with the comparative C_T method as described [12].

OPA3 protein expression

GFP fusion proteins were created by PCR amplification of the *OPA3A* and *OPA3B* coding sequences from normal human fibroblast cDNA, followed by subcloning into pEGFP-C1 and pEGFP-N1 plasmids (Clontech, Mountain View, CA). Site-directed mutagenesis was performed employing the Quick Change Site-Directed Mutagenesis Kit (Stratagene, La Jolla, CA). Specifically, the mitochondrial sorting signal (NRIKE) at residues 25-29 was replaced with the non-conserved amino acids AAAAA in the *OPA3A* and *OPA3B* containing pEGFP-N1 plasmids. The putative C-terminal peroxisomal targeting signals SKK at residues 177-179 of OPA3A and SEK at residues 178-180 of OPA3B were eliminated in the pEGFP-C1 constructs by exchanging the serine codon (TCC) at position 177 (OPA3A) or 178 (OPA3B) by a termination codon (TAA). To eliminate the mitochondrial leader sequence, the first seven residues of the leader sequence (MVVGAFP) were deleted, allowing the methionine at position 8 to function as the initiation codon in pEGFP-N1 plasmid constructs. The MitoProt (http://ihg.gsf.de/ihg/mitoprot.html) database did not predict this truncated N-terminus as a potential mitochondrial leader sequence. All plasmid constructs were verified by sequencing before use.

For localization studies, normal fibroblasts were electroporated with 3 μg of plasmid DNA in an Amaxa nucleofector electroporator (Amaxa GmbH, Walkersville, MD). Transfected fibroblasts were grown overnight on slides (Laboratory-Tek, Nalge Nunc Int., Rochester, NY), followed by fixation in 3% paraformaldehyde/phosphate-buffered saline (PBS). Some cells were treated with Mitotracker (Molecular Probes-Invitrogen, Carlsbad, CA) before fixation. Slides were then blocked/permeabilized in PBS containing 0.1% saponin, 100 μM glycine, 0.1% BSA and 2% donkey serum followed by incubation with either mouse mitochondrial antibodies (MAB 1273, Chemicon-Millipore, Billerica, MA) or rabbit PMP-70 peroxisomal antibodies (Zymed, San Francisco, CA). The cells were then washed and incubated with donkey anti-mouse secondary antibodies conjugated to cy3 or cy5 (Molecular Probes-Invitrogen, Carlsbad, CA), washed again, and mounted in VectaShield (Vector Laboratories, Burlingame, CA). Cells were imaged with a Zeiss LSM 510 META confocal laser-scanning microscope (Carl Zeiss, Microimaging Inc, Thornwood, NY) using a 488 nm Argon and a 543 nm HeNe laser. All images were acquired using a Plan NeoFluar 40X/1.3 oil DIC or a Plan Apochromat 63X/1.4 oil DIC objective. All images in Figs. 2A-C are collapsed Z-stacks (except for Fig. 2B [*g*], which is a single slice). For Fig. 2D and Supplemental Fig. S3, representative cells were imaged in a Z-stack, which were then rendered in 3-D and animated in shadow mode using AxioVision software (Carl Zeiss Vision GmbH, Thornwood, NY).

Statistical analysis

Data are presented as mean ± s.d. (Fig. 1D). Statistical analyses was performed by the two-tailed Student's *t* test of unpaired data, considering $p<0.05$ as significant (Fig. 1D).

Results and Discussion

OPA3 gene structure

Previously believed to consist of two exons and a single transcript, we now demonstrate that the *OPA3* gene (Fig. 1A) consists of 3 exons and is expressed in two transcripts, *OPA3A* (GenBank NM_025136) and *OPA3B* (GenBank NM_001017989). Both transcripts contain exon 1, which is spliced to exon 2 in *OPA3A* and exon 3 in *OPA3B*. Although cDNA studies indicate ubiquitous expression of *OPA3A* and *OPA3B*, *OPA3A* has low expression in brain and *OPA3B* has high expression in testis (Fig. 1B). The nucleotide sequences of exon 2 and exon

3, including their intron/exon boundaries, closely resemble each other, suggesting a segmental duplication event. Such duplications can be mediated by long interspersed element (LINE)-1 transposons in intronic sequences, and operate in pseudogene formation [13] and exon shuffling [14,15]. A LINE-1 (L1MC4) transposon exists in *OPA3* ~24-kb upstream of exon 2 (Fig. 1A). *OPA3A* is expressed and conserved from fungi to primates, while *OPA3B* seems to have arisen between fish and mammals (Supplemental Fig. S1).

The three known 3-MGCA type III-related mutations are all assigned to exon 2 of *OPA3A* [7,8] and its adjacent splice site [6]. We isolated fibroblast mRNA from patients with the c.143-1G>C (IVS1-1G>C) and c.320_337del (p.Q108_E113del) mutations for expression studies. Normal levels of *OPA3A* mRNA expression were found in cells with the in-frame c.320_337del deletion, while cells with the splice site mutation, c.143-1G>C, abolished fibroblast mRNA expression (Fig. 1C). In both cases, *OPA3B* expression was significantly up-regulated (Fig. 1C and D). Up-regulating one isoform to compensate for loss of another has also been described for other genes [16,17].

Subsequently, we screened DNA of 39 patients with unexplained 3-methylglutaconic aciduria and found no mutations in *OPA3*, including exon 3 (unpublished results).

OPA3 protein structure

The OPA3A and OPA3B proteins share 47 N-terminal amino acids encoded by exon 1, and their C-terminal sequences are highly homologous (Fig. 1E). The OPA3A and OPA3B proteins have no homology to other proteins, but several lines of evidence support a mitochondrial function. First, most primary optic atrophies (as seen in 3-MGCA type III patients) result from defects in mitochondria-related proteins [18,19]. Second, increased 3-MGC and 3-MGR is a common finding in mitochondrial respiratory chain disorders [20-22]. Third, mitochondrial degradation of leucine is a source of 3-MGC and 3-MGR [4,20]. Fourth, other types of 3-MGCA, i.e., type I (MIM 250950) [23], type II (MIM 30260) [24] and type V (MIM 610198) [25], are associated with mitochondrial defects.

Moreover, the first 18 amino acids that occur both in OPA3A and OPA3B have an 87.1% predicted chance of comprising an N-terminal mitochondrial leader sequence (amino acids 1-18; MitoProt, http://ihg.gsf.de/ihg/mitoprot.html). A cleavable mitochondrial leader sequence is often followed by an additional sorting/cleavage signal [26,27]; indeed, the NRIKE motif at positions 25-29 (Fig. 1E) conforms to such a prediction [26,27] (PSORTII, http://psort.nibb.ac.jp/).

OPA3 localization

Despite the above evidence for mitochondrial localization and function of OPA3, increased excretion of 3-MGC and 3-MGR can also arise from defects in non-mitochondrial pathways [28]. Regarding this possibility, it is noteworthy that OPA3A and OPA3B contain respective C-terminal tripeptides SKK and SEK (Fig. 1E), that resemble the peroxisomal targeting signal type 1 (PTS1: consensus sequence (S/A/C)(K/R/H)L) [29-31], but which have not been tested in cellular systems.

To determine the mitochondrial/peroxisomal targeting of OPA3A and OPA3B, we expressed green fluorescent protein (GFP)-tagged fusion proteins in normal fibroblasts. GFP was fused to either the C-terminus (OPA3A-GFP and OPA3B-GFP, leaving the putative mitochondrial signal free), or the N-terminus (GFP-OPA3A and GFP-OPA3B, leaving the potential peroxisomal signal free). Transfected OPA3A-GFP was distributed in a mitochondrial pattern and co-localized with a mitochondrial marker, but not a peroxisomal marker (Fig. 2A [*a* and *b*]). Even with a mutated NRIKE signal, the protein localized predominantly to mitochondria

(Fig. 2A [*c*]), but with the leader sequence disrupted as well, a more diffuse cellular distribution was seen (Fig. 2A [*d*]). With expression of GFP-OPA3A, mitochondrial localization was lost (Fig. 2B [*e*]), but the GFP co-localized with a peroxisomal marker (Fig. 2B [*f*]). This was likely aided by weakening of the N-terminal mitochondrial signal by the added GFP group. This also indicated functionality of the SKK peroxisomal sorting signal, confirmed by loss of peroxisomal localization and resumed mitochondrial localization upon deletion of the SKK signal (Fig. 2B [*g,h*]). It is possible that OPA3A only traffics to mitochondria *in vivo*, since N-terminal targeting signals take priority over C-terminal signals [32].

Like OPA3A, OPA3B localized to mitochondria (Fig. 2C [*i,k*]), but it did not localize to peroxisomes, whether or not its SEK signal was available (Fig. 2C [*j,l*]), indicating that its SEK is not a functional peroxisomal targeting signal. When OPA3B-GFP was overexpressed, large intracellular aggregates formed (Fig. 2C), perhaps due to misfolding of the amino acid variants in OPA3B compared to OPA3A. Since OPA3A deficiency results in overexpression of OPA3B, these results raised the possibility that OPA3B-induced aggregate formation contributes to the pathology of 3-MGCA type III.

Evidence for a uniquely mitochondrial role of OPA3A is also comes from proteomic databases. For instance MitoRes (http://www2.ba.itb.cnr.it/MitoNuc/;) and MITOP (http://www.mips.biochem.mpg.de/proj/medgen/mitop/) both list OPA3A as an inner mitochondrial membrane protein [33]. OPA3B was not identified in the mitochondrial proteome, perhaps due to low expression (Figure 1B) or perhaps the *OPA3B* transcript is not translated *in vivo*. Proteomic databases did not identify OPA3A or OPA3B as peroxisomal proteins (PeroxisomeDB, http://www.peroxisomeDB.org) [34].

3-MGCA type III patients' cells

Fluorescent labeling of mitochondria and peroxisomes revealed no differences in distribution, shape, size, or interactions of these organelles in fibroblasts from 3-MGCA type III patients compared with control fibroblasts (Supplemental Fig. S2). Confocal Z-series showed that peroxisomes localized uniformly throughout the cell, with a few attached to mitochondria, suggesting a conduit for metabolite exchange between the two organelles (Fig. 2D; Supplemental Fig. S3 for animated images).

Conclusion

Taken together, our findings indicate that the *OPA3* gene produces two distinct RNA transcripts, *OPA3A* and *OPA3B*. *OPA3B* has lower expression levels than *OPA3A*, and may not yield a significant translation product in human cells, since OPA3B is not identified in proteomic databases and no human disease has been associated with mutations in the *OPA3B*-specific exon 3. In addition, *OPA3A* is expressed and conserved from fungi to primates, while *OPA3B* is uniquely found in mammals (Supplemental Fig. S1). Even though *OPA3B* gene expression was significantly up-regulated in *OPA3A* deficient cells, it is likely that loss of *OPA3A* rather than gain of *OPA3B* cause disease etiology.

A potential cause of increased 3-MGC and 3-MGR is excessive shunting of organic precursors from peroxisomes to mitochondria, a process whose mechanistic basis remains enigmatic [28]. However, our cellular findings implicate that OPA3A does not localize to peroxisomes, based on its absence from peroxisomal proteomics databases [34], non-evolutionary conservation of the peroxisomal sorting signal SKK (e.g., the dog, cow, horse OPA3A proteins do not contain the C-terminal SKK sequence), and *in vivo* preference of N-terminal targeting signals over C-terminal signals [32].

We conclude that OPA3A predominantly localizes to mitochondria, which can explain the combination of elevated 3-MGC and 3-MGR [20] and optic maldevelopment and/or atrophy [18,19]. Related phenotypes (e.g., some cases of 3-MGCA type IV [4,35]) could also be caused by mitochondrial defects.

Supplementary Material

Refer to Web version on PubMed Central for supplementary material.

Acknowledgments

We thank Ian Nouvel for skillful laboratory assistance. This study was supported by the Intramural Research Program of the National Human Genome Research Institute, National Institutes of Health, Bethesda, MD, USA and by the Costeff Support Group Foundation (Y.A.).

References

[1]. Costeff H, Elpeleg O, Apter N, Divry P, Gadoth N. 3-Methylglutaconic aciduria in “optic atrophy plus”. Ann. Neurol 1993;33:103–104. [PubMed: 8494328]

[2]. Costeff H, Gadoth N, Apter N, Prialnic M, Savir H. A familial syndrome of infantile optic atrophy, movement disorder, and spastic paraplegia. Neurology 1989;39:595–597. [PubMed: 2494568]

[3]. Elpeleg ON, Costeff H, Joseph A, Shental Y, Weitz R, Gibson KM. 3-Methylglutaconic aciduria in the Iraqi-Jewish ‘optic atrophy plus’ (Costeff) syndrome. Dev. Med. Child. Neurol 1994;36:167–172. [PubMed: 7510656]

[4]. Chitayat D, Chemke J, Gibson KM, Mamer OA, Kronick JB, McGill JJ, Rosenblatt B, Sweetman L, Scriver CR. 3-Methylglutaconic aciduria: a marker for as yet unspecified disorders and the relevance of prenatal diagnosis in a ‘new’ type (‘type 4’). J. Inherit. Metab. Dis 1992;15:204–212. [PubMed: 1382150]

[5]. Nystuen A, Costeff H, Elpeleg ON, Apter N, Bonne-Tamir B, Mohrenweiser H, Haider N, Stone EM, Sheffield VC. Iraqi-Jewish kindreds with optic atrophy plus (3-methylglutaconic aciduria type 3) demonstrate linkage disequilibrium with the CTG repeat in the 3′ untranslated region of the myotonic dystrophy protein kinase gene. Hum. Mol. Genet 1997;6:563–569. [PubMed: 9097959]

[6]. Anikster Y, Kleta R, Shaag A, Gahl WA, Elpeleg O. Type III 3-methylglutaconic aciduria (optic atrophy plus syndrome, or Costeff optic atrophy syndrome): identification of the OPA3 gene and its founder mutation in Iraqi Jews. Am. J. Hum. Genet 2001;69:1218–1224. [PubMed: 11668429]

[7]. Kleta R, Skovby F, Christensen E, Rosenberg T, Gahl WA, Anikster Y. 3-Methylglutaconic aciduria type III in a non-Iraqi-Jewish kindred: clinical and molecular findings. Mol. Genet. Metab 2002;76:201–206. [PubMed: 12126933]

[8]. Ho G, Walter JH, Christodoulou J. Costeff optic atrophy syndrome: New clinical case and novel molecular findings. J. Inherit. Metab. Dis. Nov 7;2008 [Epub ahead of print].

[9]. Reynier P, Amati-Bonneau P, Verny C, Olichon A, Simard G, Guichet A, Bonnemains C, Malecaze F, Malinge MC, Pelletier JB, Calvas P, Dollfus H, Belenguer P, Malthiery Y, Lenaers G, Bonneau D. OPA3 gene mutations responsible for autosomal dominant optic atrophy and cataract. J. Med. Genet 2004;41:e110. [PubMed: 15342707]

[10]. Verny C, Amati-Bonneau P, Dubas F, Malthiery Y, Reynier P, Bonneau D. An OPA3 gene mutation is responsible for the disease associating optic atrophy and cataract with extrapyramidal signs. Rev. Neurol. (Paris) 2005;161:451–454. [PubMed: 15924081]

[11]. Davies VJ, Powell KA, White KE, Yip W, Hogan V, Hollins AJ, Davies JR, Piechota M, Brownstein DG, Moat SJ, Nichols PP, Wride MA, Boulton ME, Votruba M. A missense mutation in the murine Opa3 gene models human Costeff syndrome. Brain 2008;131:368–380. [PubMed: 18222992]

[12]. Livak KJ, Schmittgen TD. Analysis of relative gene expression data using real-time quantitative PCR and the 2(-Delta Delta C(T)) Method. Methods (San Diego, Calif 2001;25:402–408.

[13]. Ding W, Lin L, Chen B, Dai J. L1 elements, processed pseudogenes and retrogenes in mammalian genomes. IUBMB Life 2006;58:677–685. [PubMed: 17424906]

[14]. Patthy L. Genome evolution and the evolution of exon-shuffling--a review. Gene 1999;238:103–114. [PubMed: 10570989]

[15]. Babushok DV, Ostertag EM, Kazazian HH Jr. Current topics in genome evolution: molecular mechanisms of new gene formation. Cell. Mol. Life Sci 2007;64:542–554. [PubMed: 17192808]

[16]. Wang H, Ma WG, Tejada L, Zhang H, Morrow JD, Das SK, Dey SK. Rescue of female infertility from the loss of cyclooxygenase-2 by compensatory up-regulation of cyclooxygenase-1 is a function of genetic makeup. J. Biol. Chem 2004;279:10649–10658. [PubMed: 14701858]

[17]. Yu P, Li Z, Zhang L, Tagle DA, Cai T. Characterization of kynurenine aminotransferase III, a novel member of a phylogenetically conserved KAT family. Gene 2006;365:111–118. [PubMed: 16376499]

[18]. Huizing M, Brooks BP, Anikster Y. Optic atrophies in metabolic disorders. Mol. Genet. Metab 2005;86:51–60. [PubMed: 16194617]

[19]. Ferre M, Bonneau D, Milea D, Chevrollier A, Verny C, Dollfus H, Ayuso C, Defoort S, Vignal C, Zanlonghi X, Charlin JF, Kaplan J, Odent S, Hamel CP, Procaccio V, Reynier P, Amati-Bonneau P. Molecular screening of 980 cases of suspected hereditary optic neuropathy with a report on 77 novel OPA1 mutations. Hum. Mutat 2009;30:E692–705. [PubMed: 19319978]

[20]. Gibson KM, Elpeleg ON, Jakobs C, Costeff H, Kelley RI. Multiple syndromes of 3-methylglutaconic aciduria. Pediatr. Neurol 1993;9:120–123. [PubMed: 8499040]

[21]. Ibel H, Endres W, Hadorn HB, Deufel T, Paetzke I, Duran M, Kennaway NG, Gibson KM. Multiple respiratory chain abnormalities associated with hypertrophic cardiomyopathy and 3-methylglutaconic aciduria. Eur. J. Pediatr 1993;152:665–670. [PubMed: 7691603]

[22]. Scaglia F, Sutton VR, Bodamer OA, Vogel H, Shapira SK, Naviaux RK, Vladutiu GD. Mitochondrial DNA depletion associated with partial complex II and IV deficiencies and 3-methylglutaconic aciduria. J. Child Neurol 2001;16:136–138. [PubMed: 11292221]

[23]. IJlst L, Loupatty FJ, Ruiter JP, Duran M, Lehnert W, Wanders RJ. 3-Methylglutaconic aciduria type I is caused by mutations in AUH. Am. J. Hum. Genet 2002;71:1463–1466. [PubMed: 12434311]

[24]. Barth PG, Valianpour F, Bowen VM, Lam J, Duran M, Vaz FM, Wanders RJ. X-linked cardioskeletal myopathy and neutropenia (Barth syndrome): an update. Am. J. Med. Genet. A 2004;126:349–354. [PubMed: 15098233]

[25]. Davey KM, Parboosingh JS, McLeod DR, Chan A, Casey R, Ferreira P, Snyder FF, Bridge PJ, Bernier FP. Mutation of DNAJC19, a human homologue of yeast inner mitochondrial membrane co-chaperones, causes DCMA syndrome, a novel autosomal recessive Barth syndrome-like condition. J. Med. Genet 2006;43:385–393. [PubMed: 16055927]

[26]. Gavel Y, von Heijne G. Cleavage-site motifs in mitochondrial targeting peptides. Protein Eng 1990;4:33–37. [PubMed: 2290832]

[27]. Gakh O, Cavadini P, Isaya G. Mitochondrial processing peptidases. Biochim. Biophys. Acta 2002;1592:63–77. [PubMed: 12191769]

[28]. Kelley RI, Kratz L. 3-methylglutaconic acidemia in Smith-Lemli-Opitz syndrome. Pediatr. Res 1995;37:671–674. [PubMed: 7603789]

[29]. Gould SJ, Keller GA, Hosken N, Wilkinson J, Subramani S. A conserved tripeptide sorts proteins to peroxisomes. J. Cell Biol 1989;108:1657–1664. [PubMed: 2654139]

[30]. Brocard C, Hartig A. Peroxisome targeting signal 1: is it really a simple tripeptide? Biochim. Biophys. Acta 2006;1763:1565–1573. [PubMed: 17007944]

[31]. Platta HW, Erdmann R. The peroxisomal protein import machinery. FEBS Lett 2007;581:2811–2819. [PubMed: 17445803]

[32]. Neuberger G, Kunze M, Eisenhaber F, Berger J, Hartig A, Brocard C. Hidden localization motifs: naturally occurring peroxisomal targeting signals in non-peroxisomal proteins. Genome Biol 2004;5:R97. [PubMed: 15575971]

[33]. Da Cruz S, Xenarios I, Langridge J, Vilbois F, Parone PA, Martinou JC. Proteomic analysis of the mouse liver mitochondrial inner membrane. J. Biol. Chem 2003;278:41566–41571. [PubMed: 12865426]

[34]. Schluter A, Fourcade S, Domenech-Estevez E, Gabaldon T, Huerta-Cepas J, Berthommier G, Ripp R, Wanders RJ, Poch O, Pujol A. PeroxisomeDB: a database for the peroxisomal proteome, functional genomics and disease. Nucleic Acids Res 2007;35:D815–822. [PubMed: 17135190]

[35]. Neas K, Bennetts B, Carpenter K, White R, Kirk EP, Wilson M, Kelley R, Baric I, Christodoulou J. OPA3 mutation screening in patients with unexplained 3-methylglutaconic aciduria. J. Inherit. Metab. Dis 2005;28:525–532. [PubMed: 15902555]

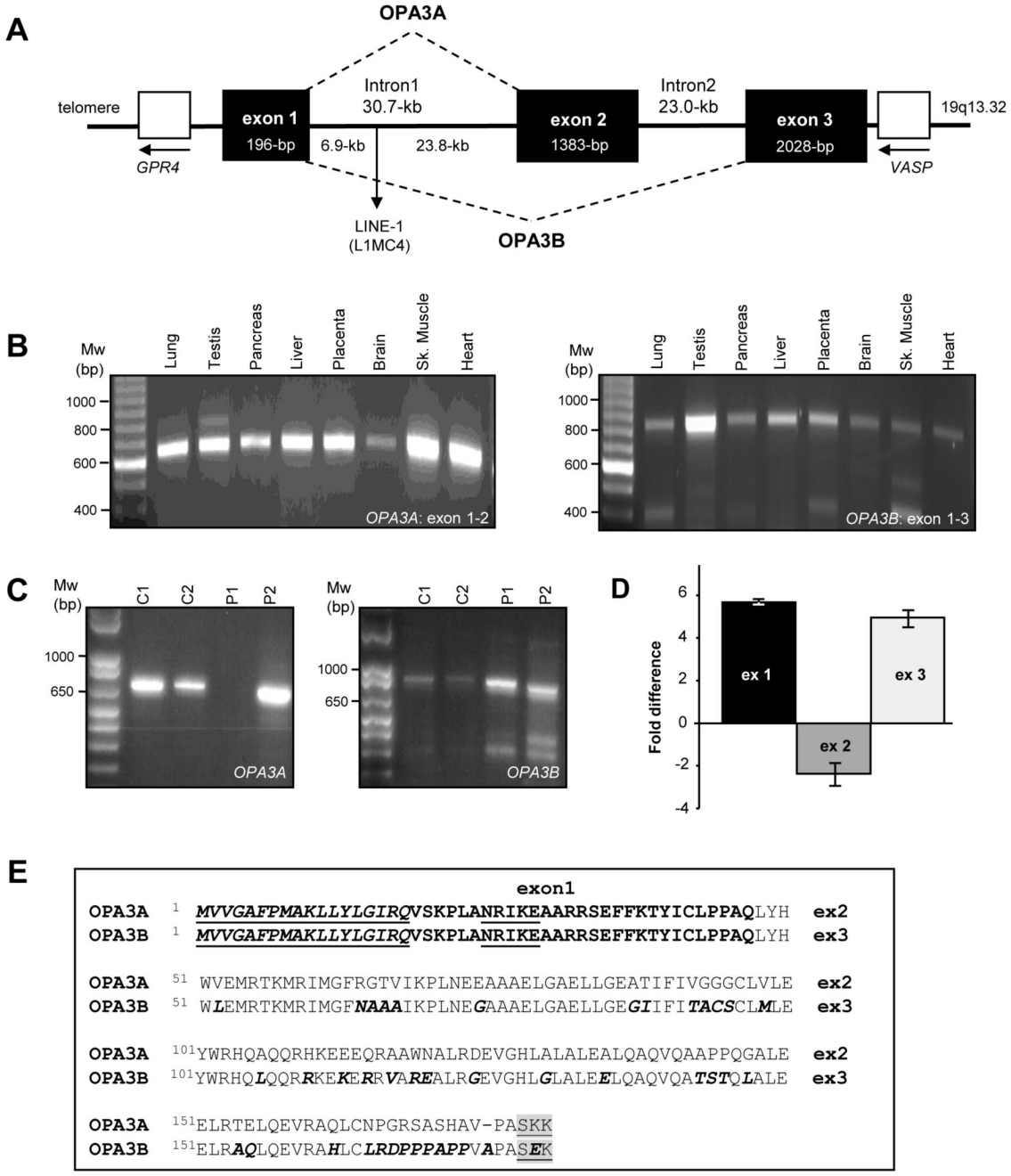

Fig. 1.

OPA3A and *OPA3B* structure and expression.

(**A**) Schematic of the *OPA3* locus on chromosome 19q13.32 (not to scale). Intron and exon sizes are indicated. Neighboring upstream and downstream genes are *GPR4* and *VASP*, respectively. A LINE-1 transposon (*L1MC4*), located about 24-kb upstream of exon 2, may have led to formation of exon 3 by segmental duplication.

(**B**) Expression analysis of *OPA3A* (left) and *OPA3B* (right) using a multiple human tissue cDNA panel.

(**C**) Expression of *OPA3A* and *OPA3B* in cDNA of normal (C1 and C2) and 3-MGCA type III fibroblasts P1 and P2, carrying homozygous c.143-1G>C and c.320-337del mutations, respectively.
(**D**) Real-time quantitative PCR analysis of *OPA3A* and *OPA3B* transcripts in 3-MGCA type III (P1) fibroblasts compared to normal fibroblasts. Exon-specific primer-probe combinations showed a 5.8 fold ($p<0.0001$) up-regulation for exon 1 (ex1), a 2.7 fold ($p=0.034$) down-regulation of exon 2 (ex2; representing *OPA3A*), and a 4.8 fold ($p<0.0001$) up-regulation of exon 3 (ex3; representing *OPA3B*) ($n=3$).
(**E**) Amino acid sequence alignment of OPA3A and OPA3B. The N-terminal amino acids encoded by exon 1 (bold) are shared by both proteins and contain a potential mitochondrial leader sequence (amino acids 1-18, underlined) and mitochondrial targeting signal NRIKE (amino acids 25-29, underlined). The potential C-terminal peroxisomal sorting signals SKK for OPA3A and SEK for OPA3B are gray shaded and underlined. Over the entire protein, OPA3A and OPA3B are 77.6% homologous; their C-terminal sequences contain 41 mismatches (printed in bold italic in the OPA3B sequence).

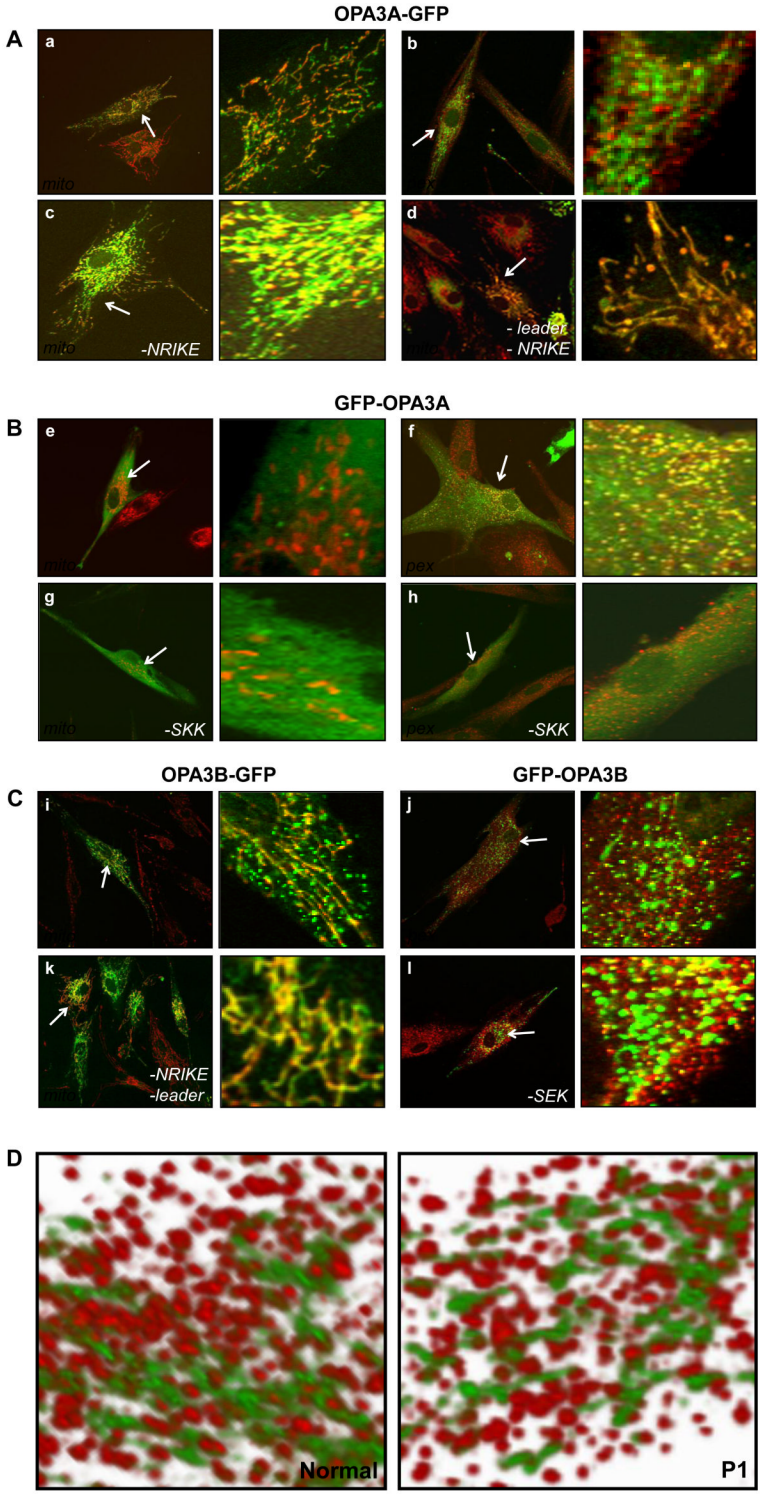

Fig. 2.

OPA3A and OPA3B intracellular localization and mitochondrial and peroxisomal distribution in normal and 3-MGCA type III fibroblasts.

OPA3A (**A, B**) and OPA3B (**C**) GFP-fusion proteins (green) were expressed in normal fibroblasts and co-stained with a mitochondrial marker (red, indicated in image as *mito*) or a peroxisomal marker (red, indicated in image as *pex*). Mutated sorting signals are indicated as - leader (disrupted mitochondrial leader sequence), -NRIKE (mutated mitochondrial targeting signal), or -SKK or -SEK (disrupted putative peroxisomal targeting signals). See text for detailed description of each image. Images in left panels are taken at low magnification (40x objective) and areas indicated by arrows are enlarged in right panels. (**D**) Mitochondria (green) and peroxisomes (red) were labeled with organelle-specific markers and imaged by confocal microscopy in a Z-stack, covering the entire cell in the Z dimension. Z-stacks were rendered in 3-D. Left panel, normal fibroblasts; right panel, 3-MGCA type III patient P1 fibroblasts (for animation, see Supplemental Fig. S3).